

Article

From Micro to Nano: Grinding Natural Magnetite Ore for Microalgae Harvesting

Michael Schobesberger¹, Simone Helmhagen¹, Stefan Mende², Sonja Berensmeier¹  and Paula Fraga-García^{1,*} 

¹ Chair of Bioreseparation Engineering, School of Engineering and Design, Technical University of Munich, Boltzmannstraße 15, 85748 Garching, Germany

² Netzsch-Feinmahltechnik GmbH, Sedanstraße 70, 95100 Selb, Germany

* Correspondence: p.fraga@tum.de

Abstract: Microalgae represent a promising feedstock for sustainable biomass and energy. The low cell concentration after cultivation, however, limits the current application fields. Magnetic microalgae harvesting is a recent approach to overcome the economic limitations of exploiting this natural resource. Accordingly, different particle types have been applied, mainly synthetically produced magnetic nanoparticles, though none on an industrial scale. Particle sizes between a few micrometers and a few nanometers have not been tested. We expected 200–500 nm to be advantageous for harvesting and as a compromise between the highly available surface and good separation properties. However, this intermediate magnetite particle size between the micro- and nano-scale cannot be reached via chemical synthesis. Therefore, we ground natural magnetite ore in a planetary ball mill and an agitator bead mill producing particles in the targeted size range. Applying ore particles ground from ~6 µm to 250 nm yields harvesting efficiencies comparable to synthetically produced nanoparticles (Ø ~ 10 nm), with only half the BET surface. Complete harvesting of saline microalgae *Microchloropsis salina* is possible with ground particles at alkaline pH. We demonstrate the feasibility of a harvesting process with natural, low-cost, easily separable, and readily available magnetite ore particles as a promising step towards exploiting valuable microalgal products in life sciences.

Keywords: iron oxide microparticles; iron oxide nanoparticles; iron ore; biomass recovery



Citation: Schobesberger, M.; Helmhagen, S.; Mende, S.; Berensmeier, S.; Fraga-García, P. From Micro to Nano: Grinding Natural Magnetite Ore for Microalgae Harvesting. *Magnetochemistry* **2023**, *9*, 149. <https://doi.org/10.3390/magnetochemistry9060149>

Academic Editors: Yongjun Xian, Jianwu Zeng and Zixing Xue

Received: 24 April 2023

Revised: 31 May 2023

Accepted: 2 June 2023

Published: 5 June 2023



Copyright: © 2023 by the authors. Licensee MDPI, Basel, Switzerland. This article is an open access article distributed under the terms and conditions of the Creative Commons Attribution (CC BY) license (<https://creativecommons.org/licenses/by/4.0/>).

1. Introduction

Producing sustainable energy and biomass for food and feed use is a significant challenge in a world with a growing population and increasing living standards. Diversification from traditional energy, food, and feed sources is necessary to secure the supply of these primary resources. Microalgae can contribute here in a sustainable way by binding carbon dioxide using solar energy to produce biomass while showing higher photosynthetic efficiencies (3–8% for microalgae, typically 0.5% for plants); in many cases, they can be grown in wastewater or seawater, microalgae cultivation does not compete with that of conventional crops, and the production can be carried out more continuously compared to plants [1–3]. With their wide range of commercial applications, microalgae have attracted much attention in recent decades. However, few processes, and only targeting high-value products, have made it to the industrial scale due to the high costs for downstream processing, especially for harvesting the microalgal biomass [4–6]. The small size of the cells in a diluted culture medium, a density similar to that of water and a high charge density on the cell walls stabilize the cellular suspension and increase costs in downstream processing [7,8]. Depending on the process, generally 20–50% but up to 90% of the total costs have to be spent on the harvesting and dewatering step, which makes most processes for microalgal products economically infeasible [5,9–12]. The conventional methods currently applied for microalgae harvesting are flocculation, flotation, and gravity settling for preprocessing, and

then centrifugation and filtration for thickening [13]. Often, some of these methods are combined to increase efficiency [14]. Gravity settling is a very simple and inexpensive method, but it is time-consuming and the resulting slurry concentration is still low. Flocculation and flotation methods are faster and low cost, but flocculants might be toxic to the biomass, also limiting the recyclability of culture medium [15]. Filtration and centrifugation allow high recovery efficiencies and very fast separation but are energy-intensive and expensive in acquisition and maintenance [16].

Another promising approach to overcome the harvesting bottleneck is using magnetic micro- and nanoparticles for cell separation and dewatering of the biomass. The idea of a magnetic separation process for biotechnological applications has often been discussed in the literature, and various potential fields have been identified and established [17,18]. The main advantages are low operating costs, high efficiency, recyclability of the particles, and simple and fast processing [7]. However, magnetic separation is not yet applied for biotech purposes on an industrial scale, due, on the one hand, to the lack of devices [17] (only one cGMP-compliant separator has been developed [19]). On the other hand, no easily separable particles are available, which show high affinity to the product, and are available in the necessary amounts at a low price.

There are two ways to produce magnetic particles in a size range between a few nanometers and a few micrometers, which we expect to be advantageous for harvesting. The bottom-up approach uses the synthesis of particles by the precipitation of iron salts, where the particles typically grow to a size of 10–30 nm [20–23]. Through agglomeration and/or sintering of these particles, larger particles up to a few micrometers can be produced for the interaction [24,25]. These particles show superparamagnetic behavior and, due to their small size, are highly adhesive to many surfaces [26]. The top-down option is to grind larger magnetite ore particles. The world's purest magnetite ore (>98%) is mined in northern Sweden in huge amounts (25.8 Mt in 2022) [27]. A high iron content of up to 72.4% makes it very attractive as a raw material for steel production and the electric industry, as the average global spot price for iron ore products is approx. USD 117 per ton (end 2022) [27]. However, during processing, the initial natural properties—especially magnetism—are lost. Within our comprehension of sustainability, we seek to use the magnetite ore with its natural and valuable characteristics, and grind it to the desired size to apply it for biotechnological separations. The grinding process is physically limited by the properties of the grinding device and economically limited by the energy input (the smaller the final mean diameter, the more expensive). Synthetically produced magnetic nanoparticles usually show saturation magnetization values in a broad range between 30 and 89 A m² kg⁻¹ [22,28–36]. The natural magnetite ore microparticles have higher saturation magnetization (91 A m² kg⁻¹) and behave remanently [37]; their magnetization values correspond to the values reported in specialized literature for the magnetism of magnetite in soils [38,39].

Our approach is to use the natural material magnetite ore to explore the use of particles larger than synthetically produced nanoparticles, because we expect easier and more complete separation in the presence of a magnetic field due to the ore's higher magnetic moment and size. Furthermore, this middle size between a few μm and a few nm represents a compromise for nutritional and, in general, other life science applications, such as the pharmaceutical and cosmetic industry: the acceptance of sizes close to the micro level is better, because they are easier to identify and separate and do not cross most of the physiological barriers. Moreover, in this work, we seek to improve the harvesting efficiency of natural magnetite ore at moderate pH by grinding the ore to submicron size, characterizing the process and the grinding products, and comparing the results to synthetically produced magnetite nanoparticles. To the best of our knowledge, we are the first to employ submicron-sized ground particles from iron ore for cell separation. We offer an explanation for the effect of the solid support surface area and concentration in the microalgae harvesting process.

2. Materials and Methods

2.1. Microalgae

The experiments were performed on *Microchloropsis salina* (SAG 40.85). The microalgae were cultivated and provided by the Chair of Biochemical Engineering of the Technical University of Munich. Cultivation took place in open thin-layer cascade photobioreactors in an artificial seawater (ASW) medium (27 g L⁻¹ NaCl, 6.6 g L⁻¹ MgSO₄ · 7 H₂O, 1.5 g L⁻¹ CaCl₂ · 2 H₂O, 1.0 g L⁻¹ KNO₃, 0.07 g L⁻¹ KH₂PO₄, 0.021 g L⁻¹ Na₂EDTA · 2 H₂O, 0.014 g L⁻¹ FeCl₃ · 6 H₂O); the ASW medium imitates the natural medium of these algae species. All chemical agents used were of analytical grade or higher. The interaction studies were conducted with microalgal cells in the stationary growth phase. The microalgal concentration after cultivation was between 10 and 25 g L⁻¹. Details on the cultivation can be found in publications by Schädler et al. [40,41]. Unless indicated otherwise, the experimental initial microalgae mass concentration was 1.0 g L⁻¹.

2.2. Magnetic Microparticles from Ore (MMO)

The magnetite microparticles from ore (MMO), product name EX009, were provided by LKAB Minerals GmbH (LKAB: Luossavaara-Kiirunavaara Aktiebolag), Essen, Germany. The particles are produced from natural iron ore mined in Malmberget, Sweden. They were stored as a dry powder (as delivered) and suspended in the medium right before usage. The size of the MMOs is very homogenous ($d_{10} = 4.8 \mu\text{m}$, $d_{50} = 5.8 \mu\text{m}$, $d_{90} = 6.9 \mu\text{m}$) (SI Figure S1). The determination was carried out using static light scattering (SLS) (Partica LA-950, Horiba Europe GmbH, Oberursel, Germany). The samples were suspended in deionized water and sonicated before measurement. The specific surface of the particles was 2.4 m² g⁻¹ and calculated from BET isotherms of nitrogen adsorption (Gemini VII, Micromeritics, Aachen, Germany). The samples were dried before measurement in the device chamber at 70 °C and 0.05 bar. Scanning electron microscopy (SEM) pictures were taken with a Philips/FEI XL 40 (FEI Company, Hillsboro, OR, USA). Light microscopic pictures were performed for size, shape, and agglomeration behavior studies with an Axio Observer 7 (Carl Zeiss AG, Oberkochen, Germany). These particles were used for the milling experiments in the planetary ball mill as well as for the agitator bead mill.

2.3. Magnetic Nanoparticles from Ore (MNO)—Preparation in a Planetary Ball Mill

For grinding in the planetary ball mill (PM100, Retsch GmbH, Haan, Germany; grinding jar and 1 mm beads made from yttrium-stabilized zirconium oxide), we chose a bead-to-ore volume ratio of 2:1 (resulting in a mass ratio of 12:1) and the addition of 25 to 30 mL of the liquid phase to obtain an engine oil-like consistency as suggested by the manufacturer. As the liquid phase, we used deionized water, ethanol, isopropanol, and 75 mM sodium phosphate buffer (pH 7.08), respectively. The grinding phases were interrupted every 10 min to cool the jar. After grinding, the beads were separated from the MNOs using a sieve, and the material was dried at 60 °C (Heraeus UT-6, Thermo Scientific GmbH, Darmstadt, Germany) until weight constancy. The phosphate ground particles were washed three times with deionized water before drying. The resulting particles were analyzed as the MMOs for particle size using SLS, for size and shape using SEM, for size and agglomeration behavior using light microscopy, and for the surface area using a BET device.

2.4. Magnetic Nanoparticles from Ore (MNO)—Preparation in an Agitator Bead Mill

MMOs were also ground in an agitator ball mill LabStar Zeta at the Netzsch application laboratory in Selb, Germany. The grinding chamber and beads (0.2–0.3 mm in diameter) were made from yttrium-stabilized zirconium oxide. The grinding chamber was filled with 1.68 kg beads, resulting in a chamber filling ratio of 85%. The initial dry mass ratio of particle suspension was 33 (w/w)%. With an increased milling time, the suspensions were diluted to a 25 (w/w)% dry mass ratio due to an increased viscosity. The agitator shaft was operated at 3200 rpm, corresponding to an agitator tip speed of 12.25 m s⁻¹. The magnetite suspension was ground for a total of 390 min in a recirculation operation with a

total net grinding energy input of 7.3 kWh. The product throughput was set to 60 kg h⁻¹ suspension, and the product temperature was kept below 30 °C. After grinding, the beads were separated, and the particles were characterized for their size using SLS, for their size and shape using SEM, for size and agglomeration behavior using light microscopy, for the surface area using a BET device, and for the Zeta potential (ZetaSizer XS, Malvern Panalytical GmbH, Kassel, Germany).

2.5. Magnetic Nanoparticle (MNP) Synthesis

Magnetic nanoparticles were synthesized according to the co-precipitation method [22]; detailed synthesis and characterization were described previously [28]. Ferric chloride and ferrous chloride are precipitated in alkaline conditions at 27 °C and under a nitrogen atmosphere. The black precipitate is washed with degassed deionized water by magnetic decantation until the conductivity is lower than 200 µS cm⁻¹. The particles grow to a size of ~10 nm but agglomerate to >100 nm and show superparamagnetic behavior with a saturation magnetization of 60 A m² kg⁻¹. The particles were stored in degassed deionized water under a nitrogen atmosphere at 4 °C until use.

2.6. Biomass Quantification

The gravimetric quantification of MMOs, MNOs and microalgae (dry weight, *DW*) was conducted in 2 mL tubes (Eppendorf, Hamburg, Germany) in 3 to 6 sample replicates. The samples were washed with deionized water three times and dried for at least 24 h at 60 °C in an oven (Heraeus UT-6, Thermo Scientific GmbH, Darmstadt, Germany). To determine the cell concentration, the optical density (*OD*) at 750 nm was measured spectrophotometrically and correlated to the gravimetric quantification of algae. The *DW/OD*₇₅₀ ratio found for *M. salina* was 0.204.

2.7. Harvesting Experiments

The harvesting experiments were conducted as follows: the microalgae and particle suspensions were prepared in the desired concentrations for the final concentrations of the experiment, e.g., 10 mL of 2 g L⁻¹ algae and 10 mL of 2 g L⁻¹ magnetite in ASW, to obtain 20 mL of 1 g L⁻¹ algae and magnetite. The suspensions were poured together, mixed, and incubated for 5 min at room temperature in an orbital shaker. The samples were then magnetically separated using strong neodymium hand magnets for another 5 min. Aliquots of the supernatant were measured spectrophotometrically. The following equation calculated the algae separation efficiency (or harvesting efficiency):

$$\text{Harvesting efficiency}[\%] = \frac{OD_0 - OD_1}{OD_0} * 100$$

where *OD*₀ corresponds to the absorbance at 750 nm before binding and *OD*₁ after binding. All experiments were performed as technical duplicates. Additional information on the harvesting experimental setup can be found in previously presented research [37].

3. Results and Discussion

3.1. Preparation of and Harvesting with MNOs

For the grinding of the magnetite ore, two types of mills were chosen. First, we present the planetary ball mill (PM 100, Retsch GmbH), which is a device for lab-scale experiments in research such as mechanochemistry, ultrafine colloidal grinding on a nanometer scale, and mixing and homogenizing soft, hard, brittle, or fibrous material. The device we used allows only batchwise processing with a maximum jar volume of 220 mL [42]. Second, we present an agitator bead mill (LabStar Zeta, Netzsch Feinmahltechnik GmbH, Selb, Germany). The laboratory mill LabStar can be operated with different grinding systems. The Zeta grinding system is designed for continuous grinding processes in recirculation mode operation. It enables the grinding of the magnetite ore down to particle sizes in the nanometer range with narrow particle size distributions. The Zeta grinding system is available

with a grinding chamber volume from 0.08 L to 400 L in different material configurations, and the upscaling of the results achieved on the laboratory scale is possible [43].

3.1.1. Planetary Ball Mill

In a planetary ball mill (PM 100, Retsch GmbH), the grinding jar is arranged eccentrically on the sun wheel of the mill. The rotation direction of the sun wheel is opposite to that of the grinding jar, so the grinding balls in the jar are subjected to superimposed rotational movement, the Coriolis force [42]. The difference in speeds between balls and jar induces frictional and impact forces, which release high dynamic energies for the size reduction of the sample. The magnetite ore was ground with 1 mm zirconia beads in different solvents (deionized water, phosphate buffer, ethanol, isopropanol) from the native size of 6 μm for 90 min until no further change in size was observed (SI Figure S2).

At the beginning of the grinding process, the two aqueous media seemed to allow faster magnetite grinding, but over time, the particles suspended in organic solvents became smaller. This can be explained by the wetting abilities of the solvents. The newly created surface needs to be stabilized in the suspension during grinding. If not, the “daughter particles” will reaggregate to minimize the surface energy. The liquid phase wets the new surface areas and separates the particles. The lower the surface tension of the solvent is, the better it will wet the surface and therefore stabilize the grinding process. The predominant frictional forces applied to the particles in a planetary ball mill lead to the abrasion of the material surface (Figure 1). Furthermore, the surface of the particles is intensely stressed during the process leading to mechanochemical modifications such as the accumulation of hydroxides on the surface [44,45]. This hydroxide-rich surface is more porous, further increasing the BET surface [46]. Therefore, the final BET surface is much bigger when an aqueous solvent is used for the particles’ grinding process (SI Figure S3).

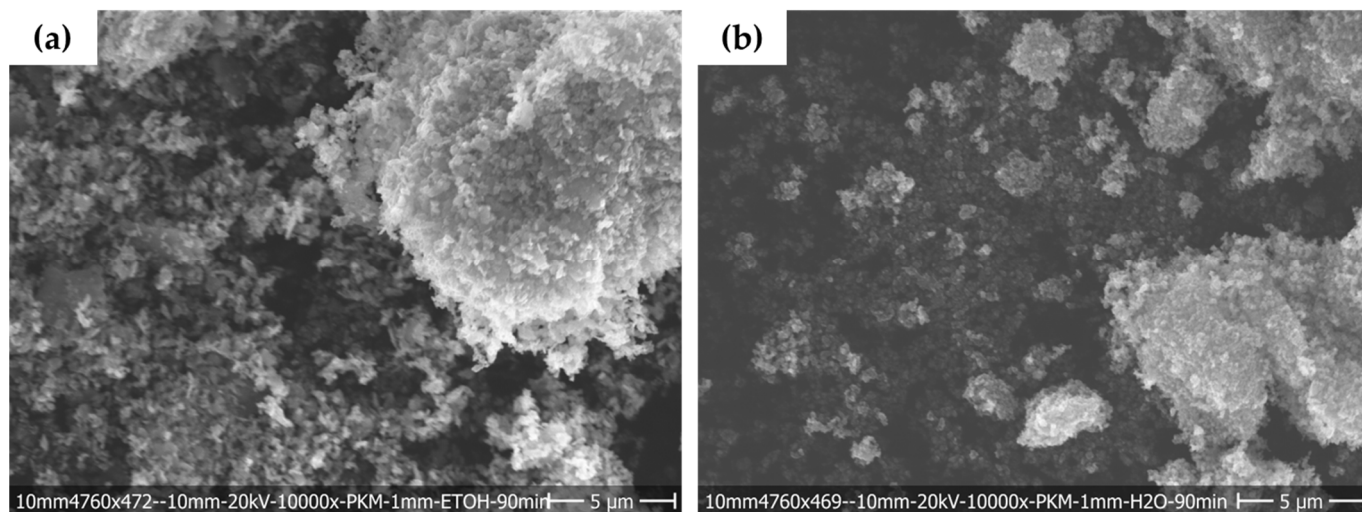


Figure 1. SEM picture of MNOs ground in the planetary ball mill while suspended in ethanol (a) and water (b). Pictures of the particles after a 90 min grinding process.

Furthermore, we observed considerable effects with particles that were ground in phosphate buffer. It is known that phosphate strongly interacts with surfaces, often stabilizing suspensions [47], and a magnetic field can influence the precipitation of phosphate salts [48]. After our grinding trials, these particles react to very weak magnetic fields in the microscope (Figure 2). We have not seen similar behavior with other particles in this work (SI Figure S4), and we only observed it with one of our microscope objectives (100 \times magnification). Additionally, we could not measure a magnetic field with our magnetometer, so we assumed a weak magnetic field below the detection limit acting on the particles. In the literature, a magnetic effect of phosphate is described, which may increase the magnetic moment of the particles while stabilizing the particles in the suspension, thus allowing an

orientation along magnetic field lines (Figure 2) [48–50]. However, the influence of this effect on the following microalgae separation process is negligible.

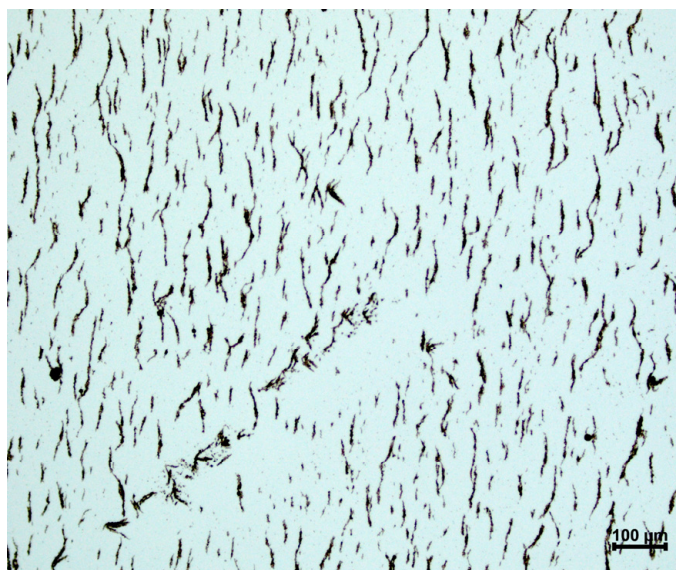


Figure 2. Brightfield image of magnetite ground in 75 mM sodium phosphate buffer for 90 min, 1 mm zirconia beads, 100× magnification.

The ground particles were used for adhesion studies when incubated with the microalgal cells. The ground particles increased the harvesting values for all pHs compared to the native magnetite ore (Figure 3).

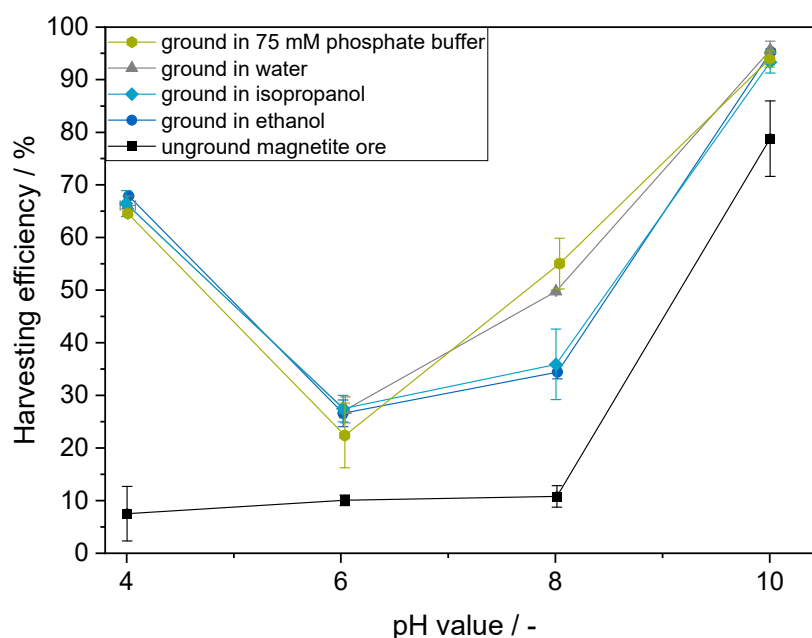


Figure 3. Harvesting efficiency with planetary ball mill ground MNOs. Particles were ground for 90 min with a bead-to-ore volume ratio of 2:1. Harvesting of 1 g L⁻¹ algae with 1 g L⁻¹ particles in ASW at room temperature, 5 min incubation time on an orbital shaker and 5 min separation time with a neodymium magnet.

Especially at acidic pH values, the interaction was much higher, caused by the higher available surface and also due to the advantageous situation for attractive electrostatic forces because of the opposite net surface charge between magnetite and the algal cells, as

can be deduced from the Zeta potential values (Figure 4). This observation is in good accordance with previous reports, which found high adsorption values in the acidic range [7,51], and in contrast to the behavior of larger particles, where we saw no harvesting enhancement at acidic pHs [37].

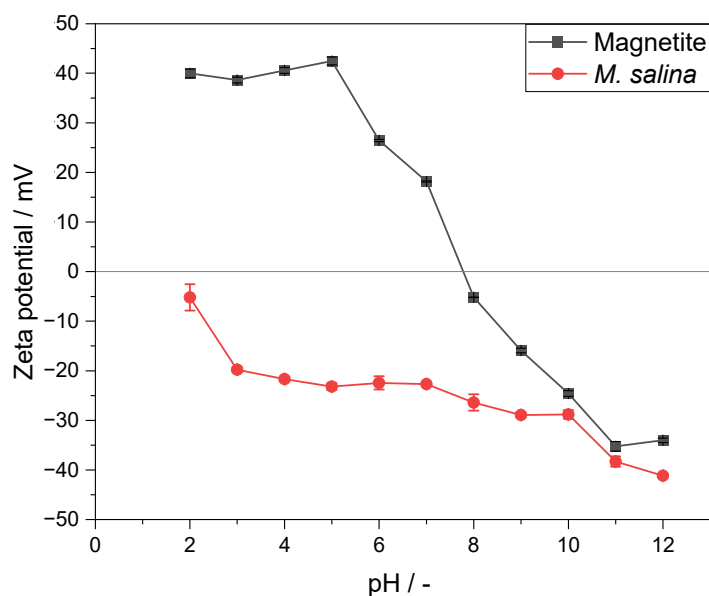


Figure 4. Zeta potential of magnetite ore particles and saline microalgae *Microchloropsis salina*.

Generally, we do not observe large differences in the harvesting efficiency for the different particles, but this is not very surprising because the size differences are also minor (they are all in the same dimension range). We are convinced that the most relevant factor for harvesting at low pHs is the size of the available surface. At pH 8, we found higher harvesting efficiencies for the samples ground in an aqueous system compared to organic solvents. Here, two effects were overlapping: the mechanochemical accumulation of hydroxides on the surface leading to a porous and therefore higher surface [44,45], and the abrasion of nanoparticles from the surface, which are then stabilized in the highly saline cultivation medium of *M. salina* (Figure 1). This offered a higher available surface for interacting with algal cells. At pH 10, the supersaturation of calcium, magnesium, phosphate and hydroxide ions causes precipitation of positively charged medium salts, mainly calcium phosphate and magnesium hydroxide. This leads to flocculation due to charge neutralization and superimposes the expected electrostatic repulsion based on the Zeta potential of magnetite and cells [37,52,53].

3.1.2. Agitator Bead Mill

Besides the planetary ball mill, we used an agitator bead mill as an alternative grinding device. In an agitator bead mill, impact forces are responsible for the dominant energy input for grinding and lead to a narrower particle size distribution compared to the planetary ball mill. This results in a higher (bulk) density and an easier separation due to a higher magnetic response because of the higher mass. In addition, with this device, continuous processing and scale-up to practically any process size are possible.

In an agitator bead mill (LabStar Zeta, Netzsch Feinmahltechnik GmbH), the sample suspension is circulated between a grinding chamber and a storage vessel. In the grinding chamber, the grinding beads are accelerated by an agitator, and impact forces between the beads and bead-wall contact mainly grind the sample particles. This continuous processing allows temperature control and monitoring of the product properties during the process without stopping it and without additional product loss. Therefore, during the process,

time-dependent characterization of the particle size, related BET surface and harvesting efficiency is possible.

With an increased grinding time, the particles becoming smaller and the surface area increases. Moreover, the freshly created surface adsorbs water from the suspension, increasing the viscosity and further influencing the grinding behavior. Therefore, after 30 min and 90 min, 500 mL of water was added to the suspension and a dilution from 33 (w/w)% to 25 (w/w)% of the magnetite suspension was achieved. After 390 min, a particle size of $d_{50} = 254$ nm (obtained from SLS measurements) was obtained (Figure 5a). SEM pictures of the particles demonstrate a homogenous particle size distribution and corroborate the expected size range; however, due to the drying process prior to SEM imaging, the samples agglomerate strongly; this effect hampers the handling as well as obtaining good contrast in the SEM images (Figure 5b). Further crushing of the particles with a consequent size reduction would be expected for longer grinding times as the curves have not reached a plateau. The necessary specific energy input to further grind the particles would, however, increase the smaller the particles become, as the collision event between particles and grinding beads becomes less frequent. Nonetheless, the particle size reached is already much smaller than with the planetary ball mill.

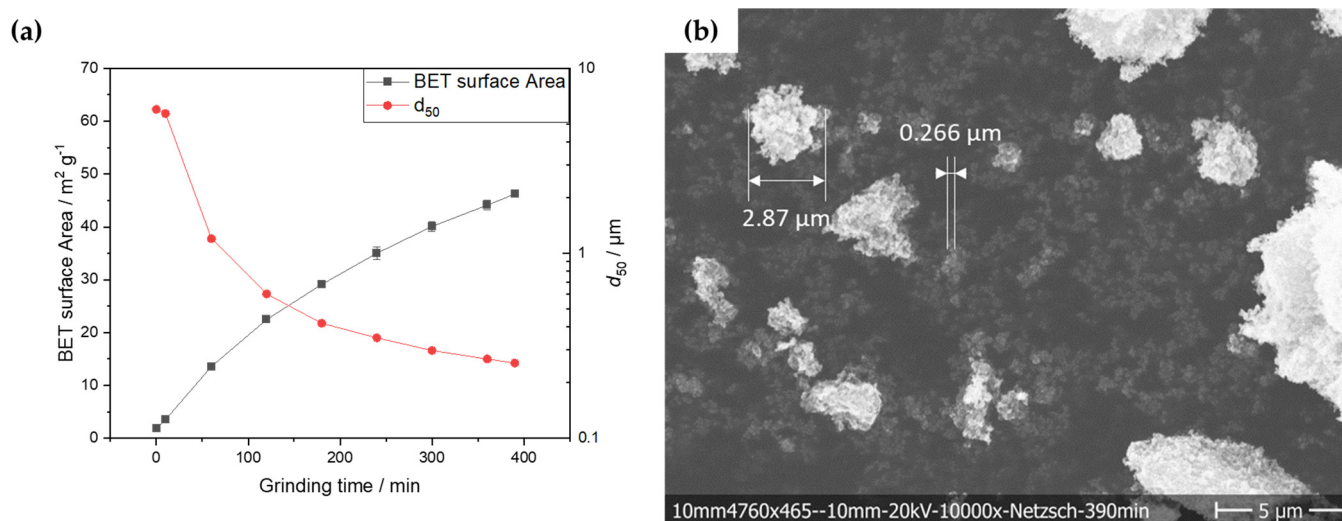


Figure 5. (a) Particle size and BET surface area during grinding of magnetite ore in an agitator bead mill (LabStar Zeta, Netzsch Feinmahltechnik GmbH); (b) SEM picture of MNOs produced after 390 min grinding in an agitator bead mill.

For the harvesting efficiencies, we found increasing values for the higher available surface and increasing pH (Figure 6). Again, the high harvesting efficiency at alkaline pH is due to the precipitation of medium components leading to flocculation. More interesting is what happens at slightly alkaline pH values: the increase in harvesting efficiency at pH 8 is much steeper than the other values. This is contradictory, as the magnetite surface starts being negatively charged at this pH, and the algae are clearly negatively charged (Figure 4). We think there is a sweet spot between the particle size and pH, where neither the particle charge nor flocculation plays the dominant role. We also observed this discrepancy in the harvesting efficiency in our planetary ball mill trials at pH 8, and the difference between organic and aqueous solvent milling. Therefore, the previously described hydroxide forming when grinding in aqueous media might also cause the difference in the harvesting efficiency [44,45]. At pH 9 and higher, the beginning precipitation of calcium phosphate and magnesium hydroxide increases the harvesting efficiency by flocculation [37].

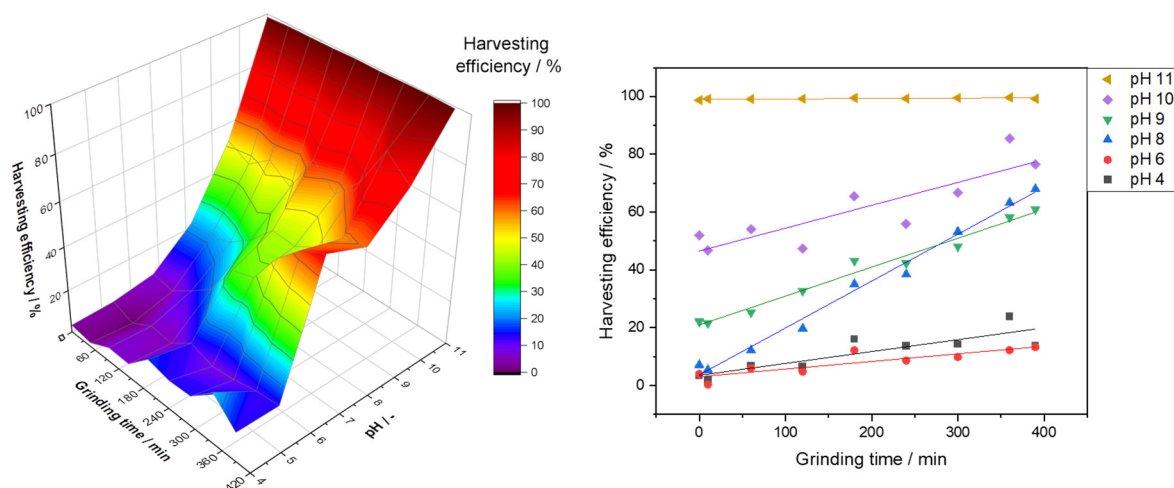


Figure 6. Harvesting efficiency over grinding time at different pH values. The original EX009 magnetite ore was ground in the agitator bead mill (LabStar, Netzsch Feinmahltechnik GmbH) for 390 min.

3.2. Magnetic Micro- vs. Nanoparticles

We compared the interaction behavior of different-sized particles: native magnetite ore EX009 (MMO; $d_{50} = 6 \mu\text{m}$), agitator bead mill ground EX009 ore (MNO; $d_{50} = 255 \text{ nm}$), and synthesized magnetite nanoparticles (MNP; $d_{50} = 13 \text{ nm}$, agglomerated $d_{50} = 120 \text{ nm}$) (Table 1). Particles obtained from planetary ball mill grinding trials have not been considered for these experiments because of the inhomogeneity in particle size distribution, BET surface, and low availability due to the small batch size. To gain better insights into the relevance of both effects, the available surface area and the total concentrations in the suspension, which we expect to both have a substantial impact on the harvesting efficiency, we compared four situations: in the first series of experiments, we kept the available surface constant and compared two different concentrations of the three particle size charges. In the second series, we used a constant particle mass for the interaction experiments with the microalgae with different types of particles again for two different concentrations.

Table 1. Harvesting efficiencies for different available surfaces and concentrations in artificial seawater at different pH values. Results are graphically illustrated for completeness in the Supporting Information (SI Figure S5).

	Particle Size d_{50} (nm)	Specific BET Surface ($\text{m}^2 \text{ g}^{-1}$)	Used Concentration (g L^{-1})	Used Surface ($\text{m}^2 \text{ L}^{-1}$)	Harvesting Efficiency in % at				
					pH 4	pH 6	pH 8	pH 10	pH 11
MNP	13–120	80	0.031	2.5	5.57	6.03	22.44	74.45	99.77
MNO	254	46	0.054	2.5	7.91	1.52	25.78	83.37	99.92
MMO EX009	5829	2.5	1	2.5	0	0	11.99	65.52	97.47
MNP	13–120	80	0.31	25	26.88	24.83	67.72	96.90	99.75
MNO	254	46	0.54	25	15.95	16.34	56.29	96.92	99.98
MMO EX009	5829	2.5	10	25	10.15	9.99	36.64	86.30	99.87
MNP	13–120	80	0.1	8	9.77	13.91	47.79	90.71	99.61
MNO	254	46	0.1	4.6	6.84	8.77	42.72	89.33	99.67
MMO EX009	5829	2.5	0.1	0.25	6.13	3.75	10.98	79.95	99.47
MNP	13–120	80	1	80	14.75	21.05	55.95	96.29	99.50
MNO	254	46	1	46	7.72	15.38	45.03	94.29	99.28
MMO EX009	5829	2.5	1	2.5	0	0	11.99	65.52	97.47

A low available surface results in similar harvesting values for all particles. The combination with alkaline flocculation at high pH leads to the previously seen complete harvesting, independent of the type of particles. It is noticeable that although the available surface is the same, the smaller the particles are, the higher the interaction at lower pH.

In this context, different effects need to be considered: agglomeration of the particles due to size effects (stronger agglomeration the smaller the particles), agglomeration due to remanence (not for MNPs), accessibility of the surface for the cells (particle on cells or cells on particle). For the ores, the accessibility of the surface is reduced because single cells block more binding spots on the magnetite in relation to the size of the cells.

In another series of experiments, we kept the mass of the added particles constant. The trend for the harvesting efficiency over pH is the same for all particles. However, the difference in the particle's harvesting efficiency is more considerable when the mass is kept constant compared to a constant surface: here, the effect of the surface is clearly recognizable. Furthermore, the effect of total concentration in the system is even stronger and would lead to even better harvesting efficiency with the nanoparticles [7]. Synthesized MNPs show the highest harvesting efficiencies but ground MNOs yield comparable results with particle diameters of ~250 nm and half of the BET surface measured. Many papers describe cell interaction with nanoparticles for microalgae harvesting [7,51,54,55]. However, most researchers focus on the synthesized particles, which only grow to 10–30 nm and agglomerate in an applied medium such as culture medium up to 150–200 nm and bigger [56,57]. The remanence is practically zero, so the superparamagnetic behavior allows very good handling in magnetic fields [22]. The interaction with surfaces as cell walls is very good as the available surface is very high. However, it is also observed that unspecific binding of different molecules occurs. This leaves a research gap for the 200–1000 nm scale, which is very interesting for applications as these particles show the same harvesting efficiency but easier identification and separation due to higher mass and magnetization. This potentially allows broader acceptance for life science applications, such as the food, cosmetic and pharmaceutical industries.

Magnetic microparticles derived from iron ore are minerally the same material as magnetite but are produced by mining iron ore bodies in Malmberget, Sweden. This material is used as crude material for steel production and is therefore available in huge amounts and at a very low cost. Several physical properties, however, differ from the nanoparticles' properties. The particle size varies between 5 μm and 150 μm (median diameter d_{50}) as supplied by the manufacturer. We further ground the material to a particle size d_{50} of ~250 nm. All those particles—ores and further processed magnetite—show remanence and agglomeration behavior but can be deagglomerated more easily compared to the synthesized nanoparticles. The higher saturation magnetization values of the natural material compared to synthesized magnetic nanoparticles [22,30,37–39] potentially allow additional applications where a higher magnetic response is essential for the separation process. Interaction behavior with foreign surfaces and molecules is comparable to the nanoparticle surface but lower in intensity, as less surface is available. Moreover, the geometry of the ore particle's surface is suspected of lowering the interaction degree between cells and the inorganic surface, as binding patterns cannot be comprehensive. Still, the harvesting efficiency of algal cells with the natural magnetite is comparable to the one of synthetically produced nanoparticles as the cell concentration after cultivation is usually low $< 1 \text{ g L}^{-1}$, and the effect of the specific surface is not crucial in this concentration range. Especially at high pH, the flocculation of cells and particles is the driving effect for harvesting. In addition to the precipitation of calcium and magnesium salts leading to the flocculation of the cells and enhancement of particle–cell adhesion, the role of extracellular polymeric substances (EPS) needs to be mentioned. As previously reported, some algal strains produce high amounts of EPS, which also increase the flocculation ability of the cells [58,59], and thus might influence the interaction with the magnetic particles. For *M. salina*, the influence of its EPS is not yet clear. The presented process for harvesting microalgae with magnetic micro- and nanoparticles derived from magnetite ore is not only applicable for the purpose presented in this work but also potentially for cell separation in general.

As a glance into the future, some critical bottlenecks still make magnetic microalgae harvesting challenging. For efficient separation and dewatering, a suitable separator needs

to be developed, which can concentrate and dewater the algae-particle slurry to a high degree. Furthermore, most of the valuable algal substances are produced intracellular, so cell disruption and product release represent another challenge. However, at least as a new option for the particle problem, microparticles from iron ore show significant advances for such applications, as they are a natural material, readily available in a scalable amount, easier to detect, separate and recycle, and are therefore expected to be the more sustainable way to realize an industrial harvesting process of microalgal cultures.

4. Conclusions

In this study, we investigate magnetic micro- and nanoparticles derived from natural magnetite ore to harvest microalgae and compare the results with synthesized magnetite nanoparticles. At pH values between 5 to 8, the influence of the size and available surface area affects the harvesting efficiency of saline microalgae *M. salina*. At higher pH values (pH > 9), the alkaline flocculation exceeds the surface influence and complete separation of the cells becomes possible. MNOs offer the same high harvesting efficiency as synthetic MNPs, and MNOs are a natural material with high availability and low cost and are therefore an excellent alternative for magnetic harvesting of microalgae. This allows the design of a process for the economic and sustainable separation of cells from complex media such as microalgae.

Supplementary Materials: The following supporting information can be downloaded at <https://www.mdpi.com/article/10.3390/magnetochemistry9060149/s1>: Figure S1: Particle size distribution for magnetite ore EX009; Figure S2: Particle size during grinding with PM100 in different solvents; Figure S3: Specific surface and SLS diameter for PM100 ground particles in different solvents; Figure S4: Microscopic pictures of magnetite particles after grinding in PM100 in different solvents; Figure S5: Harvesting efficiency of *M. salina* with different particle concentrations.

Author Contributions: Conceptualization, M.S. and P.F.-G.; methodology, M.S. and P.F.-G.; validation, M.S., S.H. and P.F.-G.; formal analysis, M.S. and S.H.; investigation, M.S., S.H. and S.M.; resources, S.B. and P.F.-G.; data curation, M.S.; writing—original draft preparation, M.S.; writing—review and editing, S.M., S.B. and P.F.-G.; visualization, M.S.; supervision, S.B. and P.F.-G.; project administration, S.B. and P.F.-G.; funding acquisition, S.B. and P.F.-G. All authors have read and agreed to the published version of the manuscript.

Funding: This research was funded by the Federal Ministry of Education and Research, grant number 031B0666A.

Institutional Review Board Statement: Not applicable.

Informed Consent Statement: Not applicable.

Data Availability Statement: The original data related used in this research can be requested at any time by contacting the corresponding author's email: p.fraga@tum.de.

Acknowledgments: We are particularly grateful to T. Schädler, A. Koruyucu, and D. Weuster-Botz (Chair of Biochemical Engineering, Technical University of Munich) for supplying us with algal biomass. We want to express our sincere gratitude to S. Viering (LKAB Minerals GmbH) for providing the MMOs, and to L. Abarca-Cabrera for providing the MNPs. The authors would also like to acknowledge J. Grosz and S. Maul for carrying out part of the harvesting experiments, M. Graf (Chair of Technical Electrochemistry, Technical University of Munich) for providing the SLS method, and M. Breidinger (Chair of Machine Elements, Technical University of Munich) for the SEM measurements. Finally, we thank C. Posten and our project partners M. Franzreb and S. Kendir (Institute of Functional Interfaces, Karlsruhe Institute of Technology) for the fruitful discussions.

Conflicts of Interest: The authors declare no conflict of interest. The funders had no role in the design of the study; in the collection, analyses, or interpretation of data; in the writing of the manuscript; or in the decision to publish the results.

References

1. Raheem, A.; Prinsen, P.; Vuppaladadiyam, A.K.; Zhao, M.; Luque, R. A review on sustainable microalgae based biofuel and bioenergy production: Recent developments. *J. Clean. Prod.* **2018**, *181*, 42–59. [CrossRef]
2. Yang, S.; Xu, J.; Wang, Z.-M.; Bao, L.-J.; Zeng, E.Y. Cultivation of oleaginous microalgae for removal of nutrients and heavy metals from biogas digestates. *J. Clean. Prod.* **2017**, *164*, 793–803. [CrossRef]
3. Hariskos, I.; Posten, C. Biorefinery of microalgae—opportunities and constraints for different production scenarios. *Biotechnol. J.* **2014**, *9*, 739–752. [CrossRef] [PubMed]
4. Yin, Z.; Zhu, L.; Li, S.; Hu, T.; Chu, R.; Mo, F.; Hu, D.; Liu, C.; Li, B. A comprehensive review on cultivation and harvesting of microalgae for biodiesel production: Environmental pollution control and future directions. *Bioresour. Technol.* **2020**, *301*, 122804. [CrossRef]
5. Singh, G.; Patidar, S.K. Microalgae harvesting techniques: A review. *J. Environ. Manag.* **2018**, *217*, 499–508. [CrossRef]
6. Mata, T.M.; Martins, A.A.; Caetano, N.S. Microalgae for biodiesel production and other applications: A review. *Renew. Sustain. Energy Rev.* **2010**, *14*, 217–232. [CrossRef]
7. Fraga-García, P.; Kubbutat, P.; Brammen, M.; Schwaminger, S.; Berensmeier, S. Bare Iron Oxide Nanoparticles for Magnetic Harvesting of Microalgae: From Interaction Behavior to Process Realization. *Nanomaterials* **2018**, *8*, 292. [CrossRef]
8. Kim, J.; Yoo, G.; Lee, H.; Lim, J.; Kim, K.; Kim, C.W.; Park, M.S.; Yang, J.-W. Methods of downstream processing for the production of biodiesel from microalgae. *Biotechnol. Adv.* **2013**, *31*, 862–876. [CrossRef]
9. Suparmaniam, U.; Lam, M.K.; Uemura, Y.; Lim, J.W.; Lee, K.T.; Shuit, S.H. Insights into the microalgae cultivation technology and harvesting process for biofuel production: A review. *Renew. Sustain. Energy Rev.* **2019**, *115*, 109361. [CrossRef]
10. Salama, E.-S.; Jeon, B.-H.; Kurade, M.B.; Abou-Shanab, R.A.; Govindwar, S.P.; Lee, S.-H.; Yang, I.-S.; Lee, D.S. Harvesting of freshwater microalgae *Scenedesmus obliquus* and *Chlorella vulgaris* using acid mine drainage as a cost effective flocculant for biofuel production. *Energy Convers. Manag.* **2016**, *121*, 105–112. [CrossRef]
11. Ummalyama, S.B.; Mathew, A.K.; Pandey, A.; Sukumaran, R.K. Harvesting of microalgal biomass: Efficient method for flocculation through pH modulation. *Bioresour. Technol.* **2016**, *213*, 216–221. [CrossRef] [PubMed]
12. Greenwell, H.C.; Laurens, L.M.L.; Shields, R.; Lovitt, R.; Flynn, K. Placing microalgae on the biofuels priority list: A review of the technological challenges. *J. R. Soc. Interface* **2009**, *7*, 703–726. [CrossRef] [PubMed]
13. Barros, A.I.; Gonçalves, A.L.; Simões, M.; Pires, J.C.M. Harvesting techniques applied to microalgae: A review. *Renew. Sustain. Energy Rev.* **2015**, *41*, 1489–1500. [CrossRef]
14. Bharte, S.; Desai, K. Techniques for harvesting, cell disruption and lipid extraction of microalgae for biofuel production. *Biofuels* **2018**, *12*, 285–305. [CrossRef]
15. Branyikova, I.; Prochazkova, G.; Potocar, T.; Jezkova, Z.; Branyik, T. Harvesting of Microalgae by Flocculation. *Fermentation* **2018**, *4*, 93. [CrossRef]
16. Mathimani, T.; Mallick, N. A comprehensive review on harvesting of microalgae for biodiesel—Key challenges and future directions. *Renew. Sustain. Energy Rev.* **2018**, *91*, 1103–1120. [CrossRef]
17. Schwaminger, S.P.; Fraga-García, P.; Eigenfeld, M.; Becker, T.M.; Berensmeier, S. Magnetic Separation in Bioprocessing Beyond the Analytical Scale: From Biotechnology to the Food Industry. *Front. Bioeng. Biotechnol.* **2019**, *7*, 233. [CrossRef]
18. Borlido, L.; Azevedo, A.M.; Roque, A.; Aires-Barros, M. Magnetic separations in biotechnology. *Biotechnol. Adv.* **2013**, *31*, 1374–1385. [CrossRef]
19. Ebeler, M.; Pilgram, F.; Wolz, K.; Grim, G.; Franzreb, M. Magnetic Separation on a New Level: Characterization and Performance Prediction of a cGMP Compliant “Rotor-Stator” High-Gradient Magnetic Separator. *Biotechnol. J.* **2017**, *13*, 1700448. [CrossRef]
20. Zhu, L.-D.; Hiltunen, E.; Li, Z. Using magnetic materials to harvest microalgal biomass: Evaluation of harvesting and detachment efficiency. *Environ. Technol.* **2017**, *40*, 1006–1012. [CrossRef]
21. Boli, E.; Savvidou, M.; Logothetis, D.; Louli, V.; Pappa, G.; Voutsas, E.; Kolisis, F.; Magoulas, K. Magnetic harvesting of marine algae *Nannochloropsis oceanica*. *Sep. Sci. Technol.* **2017**, *56*, 730–737. [CrossRef]
22. Roth, H.-C.; Schwaminger, S.P.; Schindler, M.; Wagner, F.E.; Berensmeier, S. Influencing factors in the CO₂-precipitation process of superparamagnetic iron oxide nano particles: A model based study. *J. Magn. Magn. Mater.* **2015**, *377*, 81–89. [CrossRef]
23. Wang, F.; Guo, C.; Yang, L.-R.; Liu, C.-Z. Magnetic mesoporous silica nanoparticles: Fabrication and their laccase immobilization performance. *Bioresour. Technol.* **2010**, *101*, 8931–8935. [CrossRef]
24. Dubey, V.; Kain, V. Synthesis of magnetite by coprecipitation and sintering and its characterization. *Mater. Manuf. Process.* **2017**, *33*, 835–839. [CrossRef]
25. Pospiskova, K.; Prochazkova, G.; Safarik, I. One-step magnetic modification of yeast cells by microwave-synthesized iron oxide microparticles. *Lett. Appl. Microbiol.* **2013**, *56*, 456–461. [CrossRef] [PubMed]
26. Schwaminger, S.P.; García, P.F.; Merck, G.K.; Bodensteiner, F.A.; Heissler, S.; Günther, S.; Berensmeier, S. Nature of Interactions of Amino Acids with Bare Magnetite Nanoparticles. *J. Phys. Chem. C* **2015**, *119*, 23032–23041. [CrossRef]
27. LKAB. LKAB Year-End Report 2022. 2023. Available online: <https://lkab.com/en/press/year-end-report-2022-profits-strong-but-continued-uncertainty> (accessed on 28 March 2023).
28. Abarca-Cabrera, L.; Xu, L.; Berensmeier, S.; Fraga-García, P. Competition at the Bio-nano Interface: A Protein, a Polysaccharide, and a Fatty Acid Adsorb onto Magnetic Nanoparticles. *ACS Appl. Bio Mater.* **2022**, *6*, 146–156. [CrossRef]

29. Turrina, C.; Berensmeier, S.; Schwaminger, S.P. Bare Iron Oxide Nanoparticles as Drug Delivery Carrier for the Short Cationic Peptide Lasioglossin. *Pharmaceuticals* **2021**, *14*, 405. [CrossRef]
30. Winsett, J.; Moilanen, A.; Paudel, K.; Kamali, S.; Ding, K.; Cribb, W.; Seifu, D.; Neupane, S. Quantitative determination of magnetite and maghemite in iron oxide nanoparticles using Mössbauer spectroscopy. *SN Appl. Sci.* **2019**, *1*, 1636. [CrossRef]
31. Wang, L.; Chen, T.; Cui, J.; Wei, L. Study on magnetic difference of artificial magnetite and natural magnetite. *J. Phys. Conf. Ser.* **2020**, *1699*, 012040. [CrossRef]
32. Köhler, T.; Feoktystov, A.; Petravic, O.; Kentzinger, E.; Bhatnagar-Schöffmann, T.; Feygenson, M.; Nandakumaran, N.; Landers, J.; Wende, H.; Cervellino, A.; et al. Mechanism of magnetization reduction in iron oxide nanoparticles. *Nanoscale* **2021**, *13*, 6965–6976. [CrossRef] [PubMed]
33. Mascolo, M.C.; Pei, Y.; Ring, T.A. Room Temperature Co-Precipitation Synthesis of Magnetite Nanoparticles in a Large pH Window with Different Bases. *Materials* **2013**, *6*, 5549–5567. [CrossRef]
34. Omelyanchik, A.; Kamzin, A.; Valiullin, A.; Semenov, V.; Vereshchagin, S.; Volochaev, M.; Dubrovskiy, A.; Sviridova, T.; Kozenkov, I.; Dolan, E.; et al. Iron oxide nanoparticles synthesized by a glycine-modified coprecipitation method: Structure and magnetic properties. *Colloids Surf. A Physicochem. Eng. Asp.* **2022**, *647*, 129090. [CrossRef]
35. Kemp, S.J.; Ferguson, R.M.; Khandhar, A.P.; Krishnan, K.M. Monodisperse magnetite nanoparticles with nearly ideal saturation magnetization. *RSC Adv.* **2016**, *6*, 77452–77464. [CrossRef]
36. Hadadian, Y.; Masoomi, H.; Dinari, A.; Ryu, C.; Hwang, S.; Kim, S.; Cho, B.K.; Lee, J.Y.; Yoon, J. From Low to High Saturation Magnetization in Magnetite Nanoparticles: The Crucial Role of the Molar Ratios Between the Chemicals. *ACS Omega* **2022**, *7*, 15996–16012. [CrossRef]
37. Schobesberger, M.; Real, B.K.; Meijer, D.; Berensmeier, S.; Fraga-García, P. Natural magnetite ore as a harvesting agent for saline microalgae *Microchloropsis salina*. *Bioresour. Technol. Rep.* **2021**, *15*, 100798. [CrossRef]
38. Thompson, R.; Oldfield, F. (Eds.) Magnetic properties of natural materials. In *Environmental Magnetism*; Allen & Unwin: London, UK; Boston, MA, USA; Sydney, Australia, 1986; ISBN 978-94-011-8038-2.
39. Coey, J.M.D. Magnetic properties of iron in soil iron oxides and clay minerals. In *Iron in Soils and Clay Minerals*, 217th ed.; Stucki, J.W., Goodman, B.A., Schwertmann, U., Eds.; D. Reidel Publishing Company: Dordrecht, The Netherlands, 1988; pp. 397–466. ISBN 978-94-009-4007-9.
40. Schädler, T.; Cerbon, D.C.; de Oliveira, L.; Garbe, D.; Brück, T.; Weuster-Botz, D. Production of lipids with *Microchloropsis salina* in open thin-layer cascade photobioreactors. *Bioresour. Technol.* **2019**, *289*, 121682. [CrossRef] [PubMed]
41. Schädler, T.; Neumann-Cip, A.-C.; Wieland, K.; Glöckler, D.; Haisch, C.; Brück, T.; Weuster-Botz, D. High-Density Microalgae Cultivation in Open Thin-Layer Cascade Photobioreactors with Water Recycling. *Appl. Sci.* **2020**, *10*, 3883. [CrossRef]
42. Retsch GmbH. Planeten-Kugelmühle PM 100. Available online: <https://www.retsch.de/de/produkte/zerkleinern/kugelmuehlen/planeten-kugelmuehle-pm-100/funktion-merkmale/> (accessed on 1 February 2023).
43. Netzsch Feinmahltechnik GmbH. Grinding System Zeta. Available online: <https://grinding.netzsch.com/en/products-and-solutions/wet-grinding/grinding-system-zeta> (accessed on 1 February 2023).
44. Mucsi, G. A review on mechanical activation and mechanical alloying in stirred media mill. *Chem. Eng. Res. Des.* **2019**, *148*, 460–474. [CrossRef]
45. Stenger, F.; Mende, S.; Schwedes, J.; Peukert, W. The influence of suspension properties on the grinding behavior of alumina particles in the submicron size range in stirred media mills. *Powder Technol.* **2005**, *156*, 103–110. [CrossRef]
46. Stenger, F. Grenzflächeneffekte bei der Nanozerkleinerung in Rührwerkskugelmühlen. Ph.D. Thesis, Berichte aus der Verfahrenstechnik, Shaker, Aachen, Germany, 2005; Erlangen-Nürnberg University, Aachen, Germany, 2004.
47. Tokiwa, F.; Imamura, T. Suspension stability of solid particles in the presence of various types of electrolytes. *J. Am. Oil Chem. Soc.* **1969**, *46*, 571–574. [CrossRef]
48. Sørensen, J.S.; Madsen, H.E.L. The influence of magnetism on precipitation of calcium phosphate. *J. Cryst. Growth* **2000**, *216*, 399–406. [CrossRef]
49. Baskar, S.; Ramya, J.R.; Arul, K.T.; Nivethaa, E.; Pillai, V.M.; Kalkura, S.N. Impact of magnetic field on the mineralization of iron doped calcium phosphates. *Mater. Chem. Phys.* **2018**, *218*, 166–171. [CrossRef]
50. Kuznetsov, V.; Yanovska, A.; Stanislavov, A.; Danilchenko, S.; Kalinkevich, A.; Sukhodub, L. Controllability of brushite structural parameters using an applied magnetic field. *Mater. Sci. Eng. C* **2016**, *60*, 547–553. [CrossRef] [PubMed]
51. Xu, L.; Guo, C.; Wang, F.; Zheng, S.; Liu, C.-Z. A simple and rapid harvesting method for microalgae by in situ magnetic separation. *Bioresour. Technol.* **2011**, *102*, 10047–10051. [CrossRef]
52. Ummalyma, S.B.; Gnansounou, E.; Sukumaran, R.K.; Sindhu, R.; Pandey, A.; Sahoo, D. Bioflocculation: An alternative strategy for harvesting of microalgae—An overview. *Bioresour. Technol.* **2017**, *242*, 227–235. [CrossRef] [PubMed]
53. Vandamme, D.; Foubert, I.; Fraeye, I.; Meesschaert, B.; Muylaert, K. Flocculation of *Chlorella vulgaris* induced by high pH: Role of magnesium and calcium and practical implications. *Bioresour. Technol.* **2012**, *105*, 114–119. [CrossRef]
54. Gerulová, K.; Kucmanová, A.; Sanny, Z.; Garaiová, Z.; Seiler, E.; Čaplovičová, M.; Čaplovič, L.; Palcut, M. Fe₃O₄-PEI Nanocomposites for Magnetic Harvesting of *Chlorella vulgaris*, *Chlorella ellipsoidea*, *Microcystis aeruginosa*, and *Auxenochlorella protothecoides*. *Nanomaterials* **2022**, *12*, 1786. [CrossRef]
55. Hu, Y.-R.; Wang, F.; Wang, S.-K.; Liu, C.-Z.; Guo, C. Efficient harvesting of marine microalgae *Nannochloropsis maritima* using magnetic nanoparticles. *Bioresour. Technol.* **2013**, *138*, 387–390. [CrossRef]

56. Kaveh-Baghbaderani, Y.; Allgayer, R.; Schwaminger, S.P.; Fraga-García, P.; Berensmeier, S. Magnetic Separation of Antibodies with High Binding Capacity by Site-Directed Immobilization of Protein A-Domains to Bare Iron Oxide Nanoparticles. *ACS Appl. Nano Mater.* **2021**, *4*, 4956–4963. [[CrossRef](#)]
57. Thomas, J.A.; Schnell, F.; Kaveh-Baghbaderani, Y.; Berensmeier, S.; Schwaminger, S.P. Immunomagnetic Separation of Microorganisms with Iron Oxide Nanoparticles. *Chemosensors* **2020**, *8*, 17. [[CrossRef](#)]
58. Yang, L.; Zhang, H.; Cheng, S.; Zhang, W.; Zhang, X. Enhanced Microalgal Harvesting Using Microalgae-Derived Extracellular Polymeric Substance as Flocculation Aid. *ACS Sustain. Chem. Eng.* **2020**, *8*, 4069–4075. [[CrossRef](#)]
59. Lv, J.; Guo, B.; Feng, J.; Liu, Q.; Nan, F.; Liu, X.; Xie, S. Integration of wastewater treatment and flocculation for harvesting biomass for lipid production by a newly isolated self-flocculating microalga *Scenedesmus rubescens* SX. *J. Clean. Prod.* **2019**, *240*, 118211. [[CrossRef](#)]

Disclaimer/Publisher's Note: The statements, opinions and data contained in all publications are solely those of the individual author(s) and contributor(s) and not of MDPI and/or the editor(s). MDPI and/or the editor(s) disclaim responsibility for any injury to people or property resulting from any ideas, methods, instructions or products referred to in the content.